materials

MDPI

Article

Preparation of Highly Catalytic N-Doped Carbon Dots and Their Application in SERS Sulfate Sensing

Libing Wang [1,2,3], Chongning Li [1,2,3], Yanghe Luo [1,*] and Zhiliang Jiang [1,2,3,*]

1 School of Food and Bioengineering, Hezhou University, Hezhou 542899, China; 18074841309@163.com (L.W.); lcn7882342@163.com (C.L.)
2 Key Laboratory of Ecology of Rare and Endangered Species and Environmental Protection (Guangxi Normal University), Ministry of Education, Guilin 541004, China
3 Guangxi Key Laboratory of Environmental Pollution Control Theory and Technology, Guilin 541004, China
* Correspondence: kira0217@foxmail.com (Y.L.); zljiang@mailbox.gxnu.edu.cn (Z.J.); Tel.: +86-0773-5846141 (Z.J.)

Received: 10 August 2018; Accepted: 3 September 2018; Published: 7 September 2018

Abstract: Carbon dots (CD) have excellent stability and fluorescence activity, and have been widely used in fluorescence methods. However, there are no reports about using CD as catalysts to amplify SERS signals to detect trace sulfate. Thus, preparing CD catalysts and their application in SERS sulfate-sensing are significant. In this article, highly catalytic N-doped carbon dots (CD_N) were prepared by a hydrothermal procedure. CD_N exhibited strong catalysis of the gold nanoparticle (AuNP) reaction between $HAuCl_4$ and H_2O_2. Vitoria blue 4R (VB4R) has a strong SERS peak at 1614 cm^{-1} in the formed AuNP sol substrate. When Ba^{2+} ions were added, they were adsorbed on a CD_N surface to inhibit the CD_N catalytic activity that caused the SERS peak decreasing. Upon addition of analyte SO_4^{2-}, a reaction with Ba^{2+} produced stable $BaSO_4$ precipitate and CD_N, and its catalysis recovered to cause SERS intensity increasing linearly. Thus, an SERS method was developed for the detection of 0.02–1.7 μmol/L SO_4^{2-}, with a detection limit of 0.007 μmol/L.

Keywords: N-doped carbon dots; catalysis; gold nanoreaction; SERS

1. Introduction

Because carbon dots (CD) have excellent stability, excellent chemical properties, high fluorescence activity, anti-photobleaching abilities and low cell toxicity [1–5], they are of interest to scientists. Based on the redox, complex, enzyme and immune reactions, CD have been used to determine chlorine ion, phosphate, ATP, ferric ion, hydrogen peroxide, glucose, immunoglobulin G, biological thiols, deoxyribonucleic acid, trypsin and so on [6–11]. Freire et al. [12] used polyvinyleneimine to prepare carbon quantum dots (CQDs/BPEI) to detect proteins. The nitrogen-doped carbon dots with high fluorescence efficiency have attracted much attention. Liu et al. [13] prepared nitrogen-doped graphene quantum dots and a photoelectrochemical aptasensor for chloramphenicol determination. Gu et al. [14] used 2-azidoimidazole and ammonia as reactants to prepare a fluorescent quantum dots by a thermal procedure, and to determine cysteine (Cys) by the reaction of CD-Cu^{2+}-Cys. An aptamer has good electivity and has been combined with CD. Feng et al. [15] reported a graphene quantum dots-aptamer fluorescent probe to detect lead (II) ions (as low as 0.6 nmol/L). However, there are no reports about preparation of highly catalytic N-doped carbon dots and their application to SERS quantitative analysis.

SERS is a highly sensitive and selective molecular spectral technique; it has been used in biomedical, environmental monitoring, and analytical chemistry [16–18]. Liang et al. [19] prepared silver nanorods/reduced graphene oxide (AgNR/rGO) nanosol as SERS substrate to determine

8–1500 nmol/L iodide. Yang et al. [20] prepared silver nanosol SERS substrate to determine 2–191.0 mg/L thiocyanate. Luo et al. [21] prepared triangular nanosilver based on graphene oxide catalysis, and the nanosilver was used to analysis of 0.7–72 nmol/L nitrite by SERS. Jiang et al. [22] examined the catalytic reduction of $HAuCl_4$ by cysteine with AuNP nanoenzyme to prepare gold nanosol substrate with high SERS activity to determine surfactants. Zhang et al. [23] developed a SERS method for detection of SO_2, with a detection limit of 1 mg/L, based on the Raman peak at 630 cm^{-1} of S atom. Shang et al. [24] prepared silver nanochain (AgNC) sol substrate to analyze 0.00725–0.3 μmol/L hexametaphosphate. Sulfate is one of the important anions in water science, food science, soil chemistry, biology, mineralogy and related disciplines. For analysis of trace SO_4^{2-}, there are visible–ultraviolet spectrophotometry, turbidimetry, fluorescence spectrophotometry, electrochemical analysis, radiochemical analysis, resonance Rayleigh scattering, ion chromatography, and so on [25–30]. In this experiment, highly catalytic N-doped carbon dots were prepared for the $HAuCl_4$-H_2O_2 reaction, and a new and sensitive SERS quantitative analysis method was proposed for the determination of sulfate in water and beer samples, based on the CD catalysis.

2. Materials and Methods

2.1. Apparatus and Reagents

The SERS spectra were recorded by a model of DXR smart Raman spectrometer (Thermo, Waltham, MA, USA) with laser wavelength of 633 nm, power of 3.5 mW, slit of 50 μm and acquisition time of 5 s. A model of 3K-15 high-speed refrigerated centrifuge (Sigma Co., Darmstadt, Germany) and a model of 79-1 magnetic stirrer with heating (Zhongda Instrumental Plant, Jiangsu, China) were used. A model of S-4800 field emission scanning electron microscope (Hitachi High-Technologies Corporation, Japan/Oxford Company, Oxford, UK) was used to record the graphs.

A 2.9 mmol/L $HAuCl_4$ (National Pharmaceutical Group Chemical Reagents Company, Shanghai, China), 10 μmol/L VB4R (Shanghai Reagent Three Factory, Shanghai, China) stock solution, 1 mmol/L $BaCl_2$ (Hunan Reagent Factory, Changsha, China), 1.00 mmol/L Na_2SO_4 (Xilong Science Co., Ltd., Shantou, China) and 3.4 mmoL/L trisodium citrate (Xilong Chemical Plant, Shantou, China) were prepared.

Preparation of N-doped carbon dot solution (CD_N): A 1 g of citric acid and 0, 0.5, 1.0 and 2.0 g urea were dissolved respectively in 30 mL water, and the brown yellow transparent solution was transferred to a polytetrafluoroethylene autoclave. After sealing, the autoclave was heated at 180 °C for 5 h. It was cooled to room temperature with tap water and was dialysis a night with dialysis bag of 3500 Da, and neutralized with NaOH solution to pH 7.0 to get a 0.021 g/mL CD_N that was named as CD_{0N}, $CD_{0.5N}$, CD_{1N} and CD_{2N} respectively.

2.2. Procedure

In a 5 mL graduated test tube, an appropriate amount of Na_2SO_4, 80 μL 1 mmol/L $BaCl_2$ and 75 μL 100 μg/mL CD were added and mixed well. Then 100 μL 0.1% $HAuCl_4$ and 50 μL 0.10 mol/L H_2O_2 solution were added and diluted to 1.5 mL. The tube was heated at 50 °C water bath for 20 min, cooled with ice-water, and 50 μL10 μmol/L VB4R molecular probe was added. The SERS spectrum was recorded by the spectrometer. The SERS peak intensity at 1614 cm^{-1} ($I_{1614cm^{-1}}$) and a blank $(I_{1614cm^{-1}})_0$ without SO_4^{2-} were recorded. The value of $\Delta I = I_{1614cm^{-1}} - (I_{1614cm^{-1}})_0$ was obtained.

3. Results and Discussions

3.1. Principle

The AuNP reaction was very slow, and the CD_{1N} surface contained more surface electrons that enhanced the electron transfer of the $HAuCl_4$-H_2O_2 redox reaction, and displayed strong catalytic activity on the AuNP reaction. The Ba^{2+} ions adsorb on the CD_{1N} surface and repress the catalysis.

When SO_4^{2-} was added, stable $BaSO_4$ formed and CD_{1N} was released which caused the SERS peak to increase due to formation of more SERS active gold nanoparticles. The more SO_4^{2-} was added, the more CD was released, the more Au nanoparticles formed, and the SERS signal enhanced greatly after addition of probe VB4R. Accordingly, a new SERS quantitative analysis method was proposed for trace sulfate, based on the regulation of CD_{1N} catalysis (Figure 1).

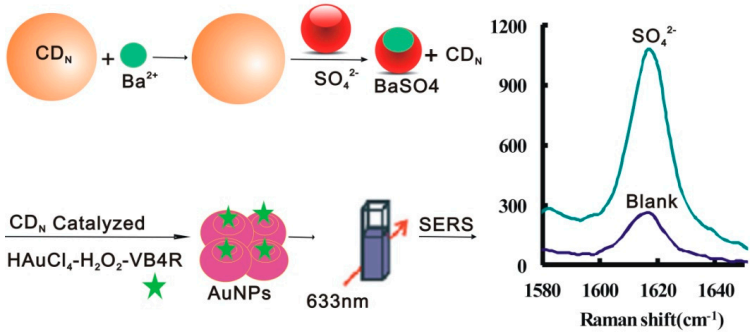

Figure 1. Surface enhanced Raman scattering (SERS) determination of sulfate by $BaSO_4$ regulation of CD_N catalysis of the gold nanoreaction between $HAuCl_4$ and H_2O_2.

3.2. SERS Spectra

Compared to common carbon nanomaterials such as graphene and C_{60}, CD are very stable and dissolved in water, and were chosen for use. The CD_{0N}, $CD_{0.5N}$, CD_{1N} and CD_{2N} analytical systems were studied by an SERS technique with VB4R molecular probes. There are nine SERS peaks at 240, 432, 675, 800, 1175, 1202, 1290, 1394 and 1614 cm^{-1} (Figure 2). With the SO_4^{2-} concentration increasing, the SERS signal increased greatly. Among the four systems, the CD_{1N} analytical system at 1614 cm^{-1} SERS peak is the most sensitive. Thus, it was chosen to detect SO_4^{2-}.

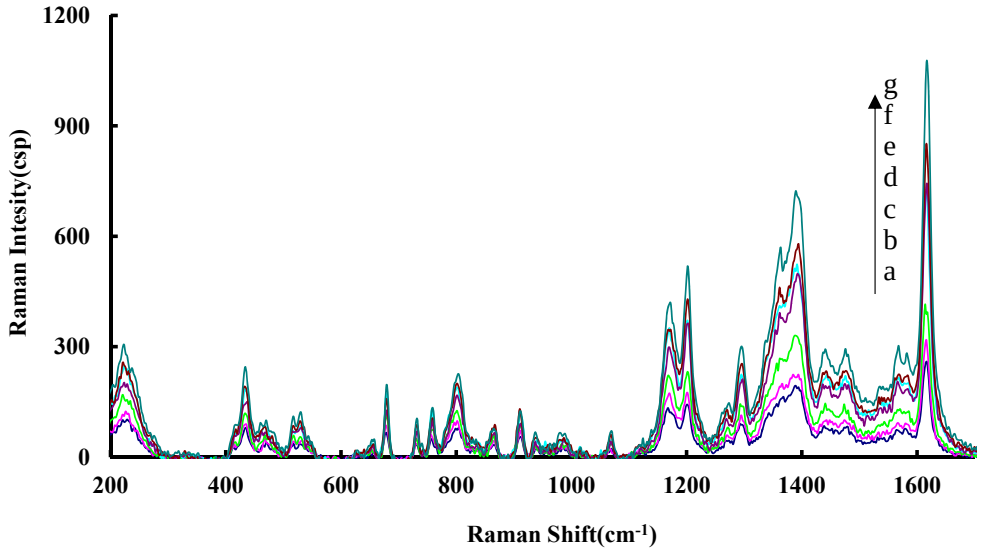

Figure 2. SERS spectrum of $HAuCl_4$-H_2O_2-CD_{1N}-Na_2SO_4-$BaCl_2$-VB4R system. (**a**): 4.2 μmol/L $HAuCl_4$ + 2.5 mol/L H_2O_2 + 5 μg/mL CD_{1N} + 53 μmol/L $BaCl_2$ + 0.33 μmol/L VB4R; (**b**): a + 0.05 μmol/L Na_2SO_4; (**c**): a + 0.10 μmol/L Na_2SO_4; (**d**): a + 0.2 μmol/L Na_2SO_4; (**e**): a + 0.7 μmol/L Na_2SO_4; (f): a + 1.0 μmol/L Na_2SO_4; (**g**): a + 1.7 μmol/L Na_2SO_4.

3.3. Scanning Electron Microscopy

Scanning electron microscopy (SEM, Hitachi High-Technologies Corporation, Japan/Oxford Company, Oxford, UK) and energy spectra of CD_{1N} show that the small CD particles are spherical

with an average size of 20 nm (Figure 3a) and the large aggregate may be the salt crystallization on the silicon wafer of SEM. There is a spectral peak at 0.25 keV for C, N and O elements. The SEM of $HAuCl_4$-H_2O_2-CD_{1N}-Na_2SO_4-$BaCl_2$-VB4R was recorded. When there is no Na_2SO_4, the $HAuCl_4$-H_2O_2 reaction is very slow to produce few quasi spherical AuNPs with an average size of 50 nm (Figure 3b); the morphology is not like the CD_{1N}, and there is a spectral peak at 1.7 keV for Au. When Na_2SO_4 was added (Figure 3c), there were more AuNPs with an average size of 40 nm owing to CD_{1N} catalysis recovering and enhancing the SERS peak. This also indicated that the particles are AuNPs in the analytical system.

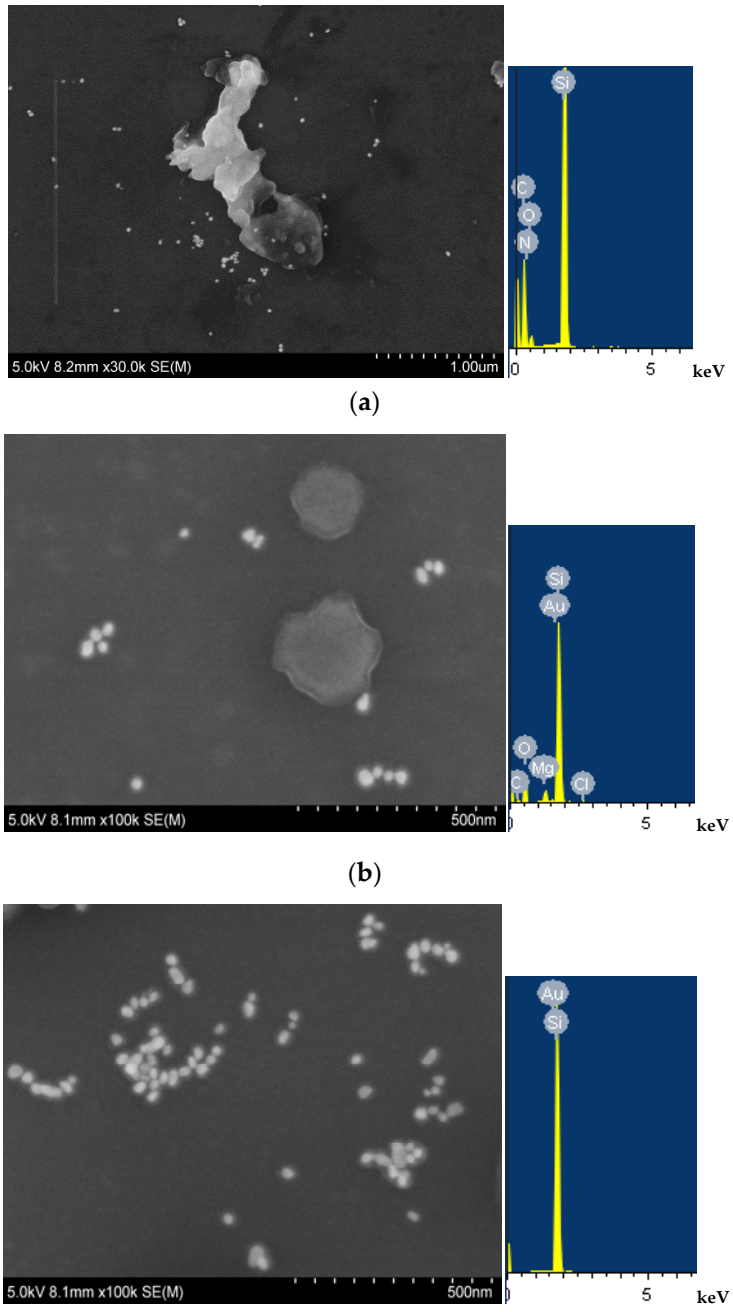

Figure 3. Scanning electron microscopy of the CD_{1N} analytical system. (**a**): 50 μg/mL CD_{1N}; (**b**): 4.2 μmol/L $HAuCl_4$ + 0.33 μmol/L VB4R + 5 μg/mL CD_{1N} + 2.5 mmol/L H_2O_2 + 53 mol/L $BaCl_2$; (**c**): b + 1.67 μmol/L Na_2SO_4.

3.4. Catalysis and Inhibition

Under the conditions as in the procedure, the AuNP reaction of H_2O_2-$HAuCl_4$ is slow. The CDN exhibited catalysis of the AuNP reaction, and the SERS intensity increased with increasing CD concentration (Table 1, Figure 4). The CD without N element exhibited weak catalysis of the AuNP reaction of H_2O_2-$HAuCl_4$, with a slope of 55.8. After doping N element such as CD_{1N} with a slope of 249, the CD_{1N} surface electrons were enhanced; the CD_{1N} surface electrons accelerated the redox electron transfer so that the gold nanoreaction was greatly enhanced to produce more AuNPs which caused the SERS intensity to increase (Figure 5).

Table 1. Comparing of the catalysis by SERS method [a].

System	Linear Range	Regress Equation	Coefficient
CD_{0N}	1.0–60 μg/mL	ΔI = 55.8x + 30	0.9898
$CD_{0.5N}$	6.0–20 μg/mL	ΔI = 89.2x + 130	0.9869
CD_{1N}	0.79–8 μg/mL	ΔI = 249.0x − 8.6	0.993
CD_{2N}	0.79–10 μg/mL	ΔI = 197.4x + 13	0.9633

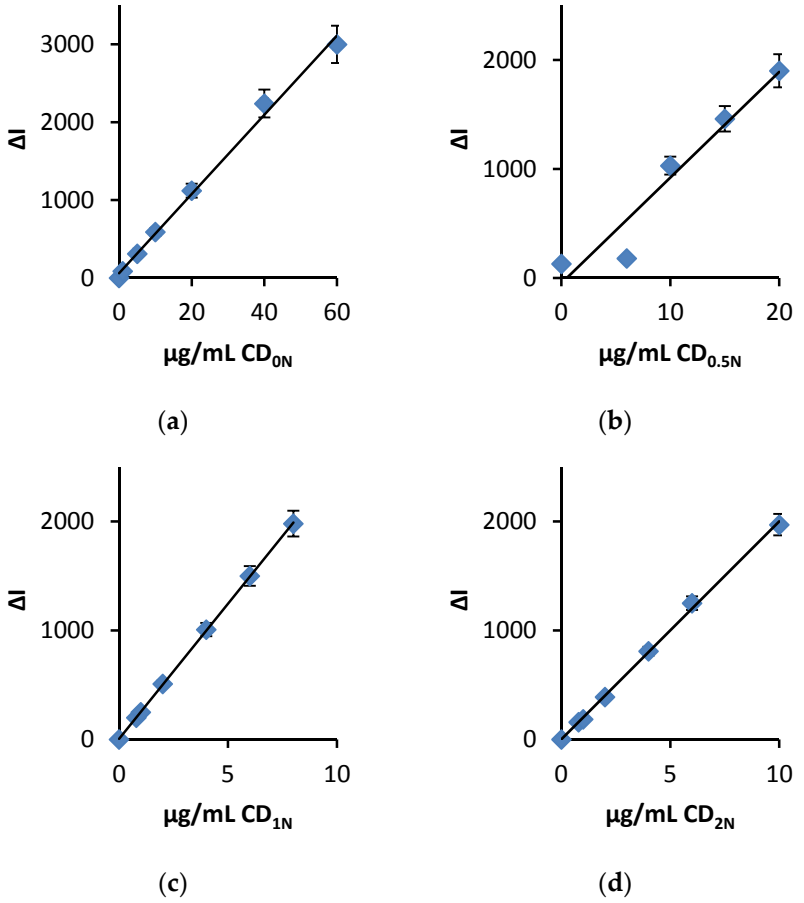

Figure 4. Relationship between the SERS intensity and CD catalyst concentration. 4.2 μmol/L $HAuCl_4$ + 2.5 mmol/L H_2O_2 + $CD_{0N–2N}$ + 0.33 μmol/L VB4R. (**a**) CD_{0N}; (**b**) $CD_{0.5N}$; (**c**) CD_{1N}; (**d**) CD_{2N}.

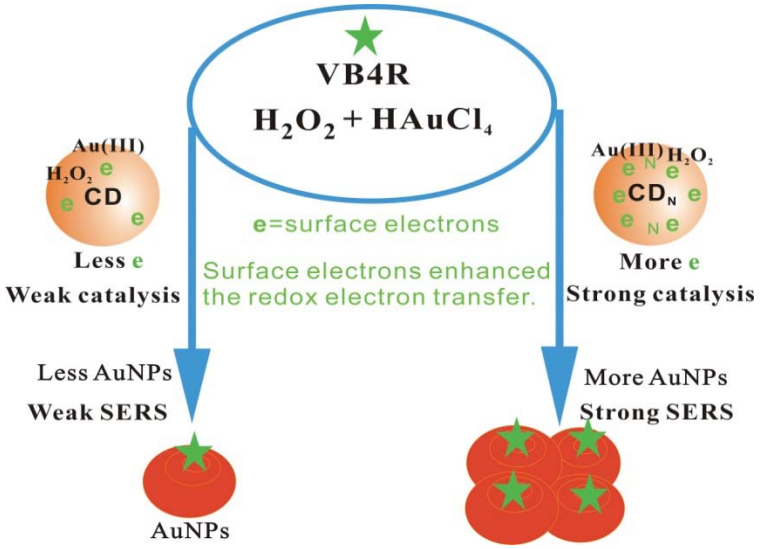

Figure 5. Enhancement of the doped N element.

3.5. Optimization of Analytical Conditions

The effect of reagent concentration such as $HAuCl_4$, H_2O_2, CD_{1N}, $BaCl_2$ and VB4R, reaction temperature and time were optimized, respectively (Figure 6). When $HAuCl_4$ is 4.2 μmol/L, most AuNPs formed in analytical systems with large Δ*I*. With increasing H_2O_2, the Δ*I* increased due to the formed AuNPs increasing, and a 2.5 mmol/L H_2O_2 gives the largest Δ*I*. CD_{1N} is the catalyst of the AuNP reaction, when the catalyst concentration increased, the Δ*I* enhanced, a 5 μg/mL CD_{1N} gives the largest Δ*I*. $BaCl_2$ can inhibit the CD catalysis, when its concentration increased the Δ*I* was enhanced due to the blank decreasing, a 53 μmol/L $BaCl_2$ gives the largest Δ*I*. VB4R is a sensitive molecular probe; when the concentration increased the Δ*I* enhanced due to more VB4R adsorption on the AuNP surface, a 0.33 μmoL/L VB4R gives biggest Δ*I*. Reaction temperature and time were considered; 50 °C for 20 min gives biggest Δ*I*. Thus, a 4.2 μmol/L $HAuCl_4$, 2.5 mmol/L H_2O_2, 5 μg/mL CD_{1N}, 53 μmol/L $BaCl_2$ and 0.33 μmoL/L VB4R, and a reaction temperature of 50 °C for 20 min was selected in this SERS method.

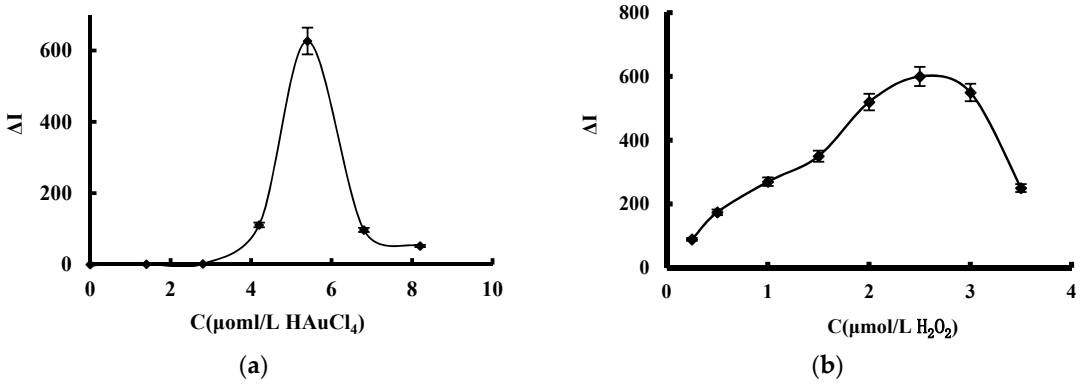

Figure 6. *Cont.*

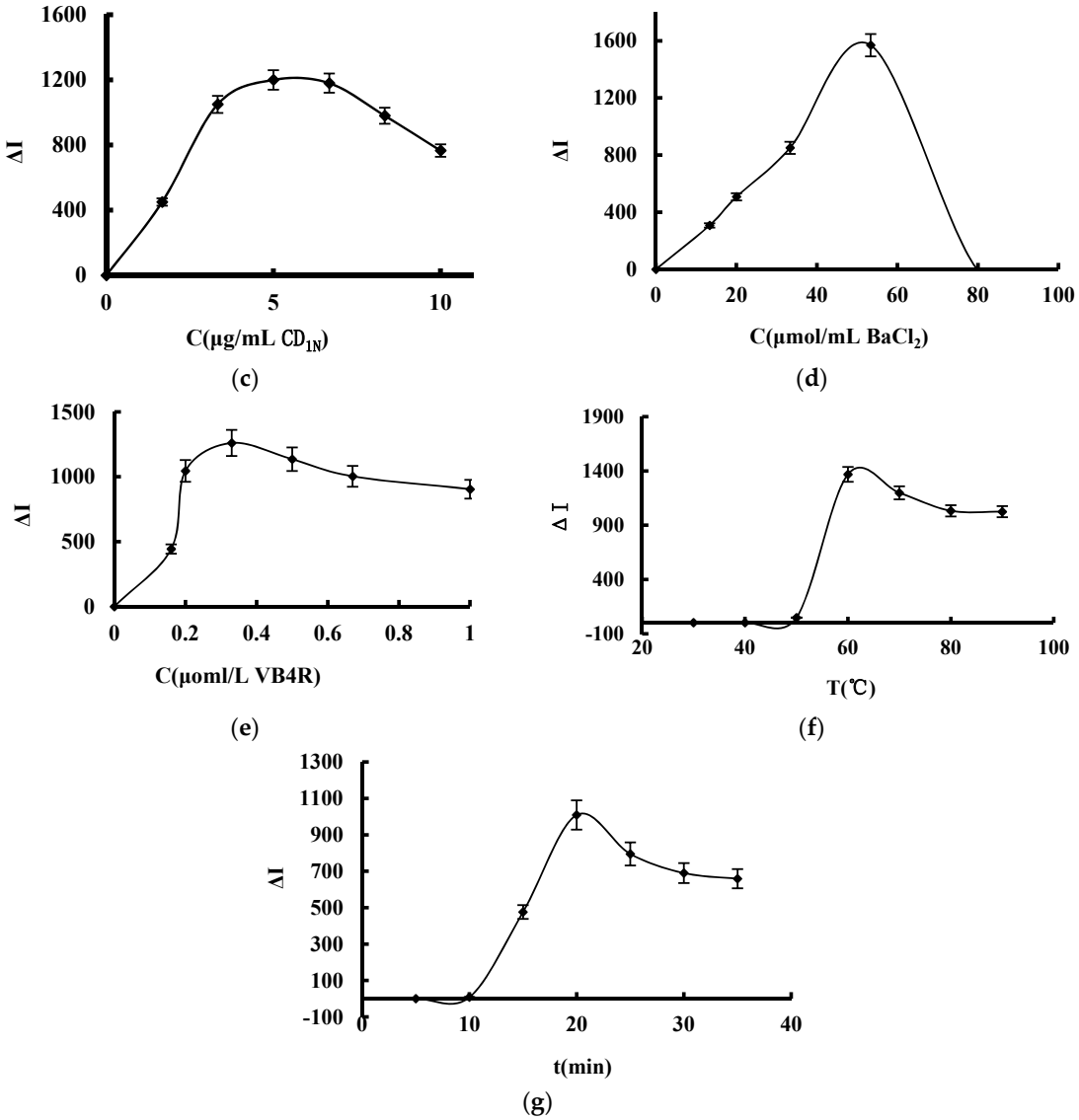

Figure 6. Effect of reagent concentration, reaction temperature and time. (**a**): $HAuCl_4$ + 2.5 mmol/L H_2O_2 + 5 μg/mL CD_{1N} + 0.67 μmol/L Na_2SO_4 + 53 μmol/L $BaCl_2$ + 0.33 μmol/L VB4R; (**b**): 4.2 μmol/L $HAuCl_4$ + 0.33 μmol/L VB4R + 5 μg/mL CD_{1N} + 0.67 μmol/L Na_2SO_4 + 53 μmol/L$BaCl_2$; (**c**): 4.2 μmol/L $HAuCl_4$ + 2.5 mmol/L H_2O_2 + CD_{1N} + 0.67 μmol/L Na_2SO_4 + 53 μmol/L $BaCl_2$ + 0.33 μmol/L VB4R; (**d**): 4.2 μmol/L $HAuCl_4$ + 2.5 mmol/L H_2O_2 + 5 μg/mL CD_{1N} + 0.67 μmol/L Na_2SO_4 + $BaCl_2$ + 0.33 μmol/L VB4R; (**e**): 4.2 μmol/L $HAuCl_4$ + 2.5 mmol/L H_2O_2 + 5 μg/mL CD_{1N} + 0.67 μmol/L Na_2SO_4 + 53 μmol/L $BaCl_2$ + VB4R; (**f**): Reaction temperature, 4.2 μmol/L $HAuCl_4$ + 2.5 mmol/L H_2O_2 + 5 μg/mL CD_{1N} + 0.67 μmol/L Na_2SO_4 + 53 μmol/L $BaCl_2$ + 0.33 μmoL/L VB4R; (**g**): Reaction time, 4.2 μmol/L $HAuCl_4$ + 2.5 mmol/L H_2O_2 + 5 μg/mL CD_{1N} + 0.67 μmol/L Na_2SO_4 + 53 μmol/L $BaCl_2$ + 0.33 μmoL/L VB4R.

3.6. Performance Curve

The working curve of the system was drawn according to the experimental method. In the four systems (Table 2, Figure 7), the CD_{1N} was most sensitive, with a linear range (LR) of 0.02–1.7 μmol/L and a detection limit (DL) of 0.007 μmol/L, and was selected for detection of sulfate. Comparison of the reported methods for detection of sulfate [25–30] showed the SERS method was more sensitive. The C_{60} catalytic SERS method was used to detect sulfate, but the preparation of C_{60} is complex, the C_{60} nanosol is unstable [25], and the CD_{1N} analytical system overcomes the disadvantages.

Table 2. Analytical features of CD-catalytic SERS determination of sulfate.

CD	Linear Equation	Coefficient	LR (μmol/L)	DL(μmol/L)
CD_{0N}	ΔI = 66.9C + 20.4	0.9283	1.0–6.0	0.50
$CD_{0.5N}$	ΔI = 166.4C + 48.8	0.9463	0.5–2.31	0.20
CD_{1N}	ΔI = 348.8C + 18.0	0.9384	0.02–1.7	0.007
CD_{2N}	ΔI = 268.6C−73.9	0.9403	0.06–2.66	0.02

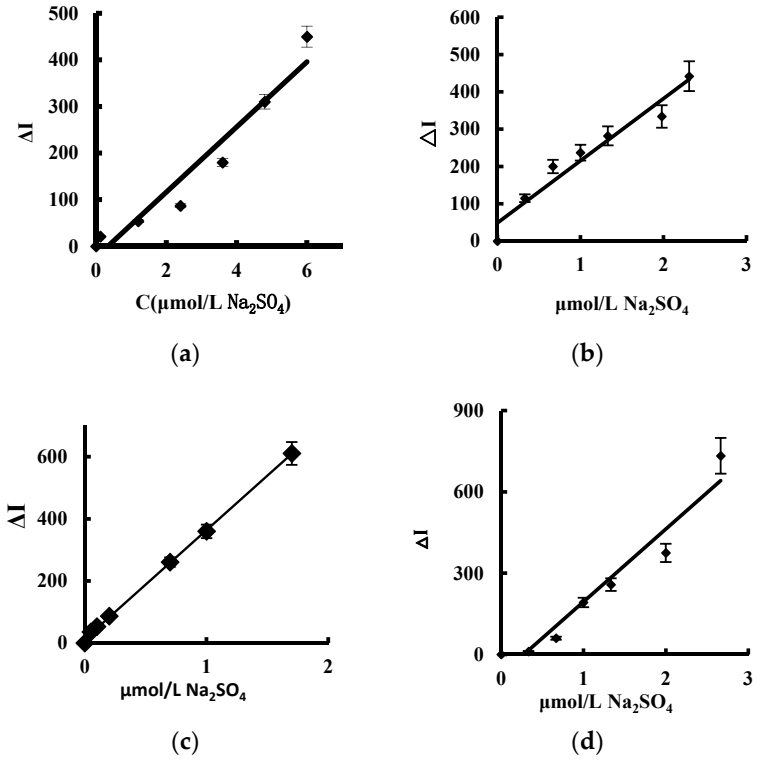

Figure 7. Working curves for CD catalytic-SERS method. 4.2 μmol/L $HAuCl_4$ + 2.5 mmol/L H_2O_2 + 5 μg/mL CD + 53 μmol/L $BaCl_2$ + 0.33 μmol/L VB4R. (**a**): CD_{0N}; (**b**): $CD_{0.5N}$; (**c**): CD_{1N}; (**d**): CD_{2N}.

3.7. Influence of Foreign Substances

The influence of foreign substance on the determination of 0.66 μmol/L SO_4^{2-} was investigated according to the experimental method. When the relative error is within 10%, results show that 33 μmol/L Na^+, Zn^{2+}, Ca^{2+}, ethanol, Pb^{+2}, NH_4^+, K^+, SO_3^{2-}, Bi^{3+} and Cu^{+2}, 26.4 μmol/L HCO_3^-, Mg^{2+}, 16.5 μmol/L ethylene glycol, 6.6 μmol/L Cr^{6+}, Fe^{3+}, NO_2^- and glycolic acid did not interfer with the SERS detection. Table 3 shows that the SERS quantitative analysis method has good selectivity.

Table 3. Effect of interfering substances on the SERS detection of 0.66 μmol/L SO_4^{2-}.

Foreign Substance	Tolerance Concentration (μmol/L)	Relative Error (%)	Foreign Substance	Tolerance Concentration (μmol/L)	Relative Error (%)
Na^+	33	5.0	Cu^{2+}	33	7.6
Zn^{2+}	33	6.4	HCO_3^-	26.4	8.6
Ca^{2+}	33	−6.7	Mg^{2+}	26.4	6.0
ethanol	33	−5.6	ethylene glycol	16.5	5.8
Pb^{2+}	33	7.0	Cr^{6+}	6.6	−6.0
NH_4^+	33	3.9	Fe^{3+}	6.6	−4.5
K^+	33	6.0	NO_2^-	6.6	6.2
SO_3^{2-}	33	−7.9	glycolic acid	6.6	5.0
Bi^{3+}	33	6.4			

3.8. Analysis of Samples

The water samples including tap water, Rong lake water and Shan lake water were taken into sample bottles. The lake water was filtered with filter paper, and then a 2.0 mL water sample was removed in a centrifuge tube. Three beer samples were purchased supermarkets. Samples were centrifuged at 7000 r/min for 10 min, to obtain a sample solution. The sulfate content was determined according to the SERS detection procedure. The SERS results were in agreement with that of ion chromatography (IC), the relative standard deviation was in the range of 0.90–4.77% and the recovery was between 92.3% and 105% (Table 4).

Table 4. Analytical results of sulfate in water samples.

Sample	Single Value (μmol/L)	Average (μmol/L)	Added (μmol/)	Found (μmol/L)	Recovery (%)	RSD (%)	Content (μmol/L)	IC Results (μmol/L)
Running water	0.39, 0.41, 0.38, 0.40, 0.43	0.40	0.13	0.52	92.3	4.77	0.40	0.38
Ronng lake water	1.12, 1.17, 1.11, 1.17, 1.17	1.15	0.13	1.274	95	2.6	1.15	1.22
Shan lake water	0.70, 0.71, 0.71, 0.72, 0.71	0.71	0.13	0.839	99.2	0.90	0.71	0.68
Beer 1	1.22, 1.26, 1.30, 1.28, 1.32	1.28	0.20	1.47	95	3.0	1.28	1.20
Beer 2	1.30, 1.35, 1.38, 1.39, 1.33	1.35	0.20	1.56	105	2.7	1.35	1.38
Beer 3	1.39, 1.30, 1.39, 1.32, 1.25	1.33	0.20	1.52	95	4.3	1.33	1.28

4. Conclusions

Highly catalytic CD_N was prepared by a hydrothermal procedure, and it was used to catalyze the reduction of chlorauric acid by H_2O_2 to produce AuNP sol substrate with high SERS activity. Ba(II) ions can combined with CD_N to inhibit the catalysis of CD_N. Upon addition of sulfate ions, stable barium sulfate precipitates formed, and CD_N was released, which causes CD_N catalysis to be activated and the SERS signal to be enhanced. Based on this principle, a new, simple and selective SERS quantitative analysis method was established for the detection of trace sulfate.

Author Contributions: C.L. and L.W. finished the work, acquired data, plotted Figures 1–7 and drafted the manuscript. Y.L. and Z.J. designed the work, analyzed data, and revised the manuscript.

Funding: This research was funded by the National Natural Science Foundation of China [grant number 21667006, 21767004, 21465006, 21477025].

Conflicts of Interest: All authors declare no conflict of interest.

References

1. Dong, Y.Q.; Chen, C.Q.; Zheng, X.T.; Gao, L.L.; Cui, Z.M.; Yang, H.B.; Guo, C.X.; Chi, Y.W.; Li, C.M. One-step and high yield simultaneous preparation of single-and multi-layer graphene1 quantum dots from CX-72 carbon black. *J. Mater. Chem.* **2012**, *22*, 8764–8766. [CrossRef]
2. Shen, J.H.; Zhu, Y.H.; Yang, X.L.; Li, C.Z. Graphene quantum dots: Emergent nanolights for bioimaging, sensors, catalysis and photovoltaic devices. *Chem. Commun.* **2012**, *48*, 3686–3699. [CrossRef] [PubMed]
3. Lu, J.; Yeo, P.S.; Gan, C.K.; Wu, P.; Loh, K.P. Transforming C_{60} molecules into graphene quantum dots. *Nat. Nanotechnol.* **2011**, *6*, 247–252. [CrossRef] [PubMed]
4. Liu, R.; Wu, D.; Feng, X.; Müllen, K. Bottom-up fabrication of photoluminescent graphene quantum dots with uniform morphology. *J. Am. Chem. Soc.* **2011**, *133*, 15221–15223. [CrossRef] [PubMed]
5. Niu, Z.; Chen, J.; Hng, H.H.; Ma, J.; Chen, X. A leavening strategy to prepare reduced graphene oxide foams. *Adv. Mater.* **2012**, *24*, 4144–4150. [CrossRef] [PubMed]

6. Dong, Y.; Li, G.; Zhou, N.; Wang, R.; Chi, Y. Graphene quantum dot as a green and facile sensor for free chlorine in drinking water. *Anal. Chem.* **2012**, *84*, 8378–8382. [CrossRef] [PubMed]
7. Bai, J.M.; Zhang, L.; Liang, R.P.; Qiu, J.D. Graphene quantum dots combined with europium ions as photoluminescent probes for phosphate sensing. *Chem. Eur. J.* **2013**, *19*, 3822–3826. [CrossRef] [PubMed]
8. Liu, J.J.; Zhang, X.L.; Cong, Z.X.; Chen, Z.T.; Yang, H.H.; Chen, G.N. Glutathione-functionalized graphene quantum dots as selective fluorescent probes for phosphate-containing metabolites. *Nanoscale* **2013**, *5*, 1810–1815. [CrossRef] [PubMed]
9. Wang, D.; Wang, L.; Dong, X.; Shi, Z.; Jin, J. Chemically tailoring graphene oxides into fluorescent nanosheets for Fe^{3+} ion detection. *Carbon* **2012**, *50*, 2147–2154. [CrossRef]
10. Zhang, Y.; Wu, C.; Zhou, X.; Wu, X.; Yang, Y.; Wu, H.; Guo, S.; Zhang, J. Graphene quantum dots/gold electrode and its application in living cell H_2O_2 detection. *Nanoscale* **2013**, *5*, 1816–1819. [CrossRef] [PubMed]
11. Li, J.; Li, P.; Zhang, L.; Dong, C. Recent progress in the performance improvement of carbon nanodots. *J. Anal. Sci.* **2018**, *34*, 429–436.
12. Freire, R.M.; Le, N.D.B.; Jiang, Z.W.; Kim, C.S.; Rotello, V.M.; Fechine, P.B.A. NH_2-rich Carbon Quantum Dots: A protein-responsive probe for detection and identification. *Sens. Actuators B* **2018**, *255*, 2725–2732. [CrossRef]
13. Liu, Y.; Yan, K.; Okoth, O.K.; Zhang, J.D. A label-free photoelectrochemical aptasensor based on nitrogen-doped graphene quantum dots for chloramphenicol determination. *Biosens. Bioelectron.* **2015**, *74*, 1016–1021. [CrossRef] [PubMed]
14. Gu, T.T.; Zou, W.; Gong, F.C.; Xia, J.Y.; Chen, C.; Chen, X.J. A specific nanoprobe for cysteine based on nitrogen-rich fluorescent quantum dots combined with Cu^{2+}. *Biosens. Bioelectron.* **2017**, *100*, 79–84. [CrossRef] [PubMed]
15. Zhao, S.Q.; Xiao, Y.S.; Lu, J.C.; Jian, R.C.; Hui, F. A fluorescent nanosensor based on graphene quantum dots–aptamer probe and graphene oxide platform for detection of lead (II) ion. *Biosens. Bioelectron.* **2015**, *68*, 225–231.
16. Wang, A.X.; Kong, X. Review of Recent Progress of Plasmonic Materials and Nano-Structures for Surface-Enhanced Raman Scattering. *Materials* **2015**, *8*, 3024–3052. [CrossRef] [PubMed]
17. Wang, L.; Zhang, Y.; Yang, Y.; Zhang, J. Strong dependence of surface enhanced raman scattering on structure of graphene oxide film. *Materials* **2018**, *11*, 1199. [CrossRef] [PubMed]
18. Ouyang, H.; Li, C.; Liu, Q.; Wen, G.; Liang, A.; Jiang, Z. Resonance Rayleigh scattering and SERS spectral detection of trace Hg(II) based on the gold nanocatalysis. *Nanomaterials* **2017**, *7*, 114. [CrossRef] [PubMed]
19. Liu, Q.; Zhang, X.; Wen, G.; Luo, Y.; Liang, A.; Jiang, Z. A sensitive silver nanorod/reduced graphene oxide SERS analytical platform and its application to quantitative analysis of iodide in solution. *Plasmonics* **2015**, *10*, 285–295. [CrossRef]
20. Yang, Q.Q.; Liang, F.H.; Wang, D.; Ma, P.Y.; Gao, D.J.; Han, J.Y.; Li, Y.L.; Yu, A.A.; Song, D.Q.; Wang, X.H. Simultaneous determination of thiocyanate ion and melamine in milk and milk powder using surface-enhanced Raman spectroscopy. *Anal. Methods* **2014**, *6*, 8388–8395. [CrossRef]
21. Luo, Y.; Wen, G.; Dong, J.; Liu, Q.; Liang, A.; Jiang, Z. SERS detection of trace nitrite ion in aqueous solution based on the nitrosation reaction of rhodamine 6G molecular probe. *Sens. Actuators B* **2014**, *201*, 336–342. [CrossRef]
22. Liang, A.; Wang, X.; Wen, G.; Jiang, Z. A sensitive and selective Victoria blue 4R SERS molecular probe for sodium lauryl sulfate in AuNP/AgCl sol substrate. *Sens. Actuators B* **2017**, *244*, 275–281. [CrossRef]
23. Zhang, L.; Zeng, Y.M.; Zhao, J.J.; Chen, H.J.; Kong, J.L.; Chen, Q.Z.; Lin, H.Z.; Tian, Z.Q.; Liu, G.K. Rapid determination of sulfur dioxide residues in foods based on surface-enhanced Raman spectroscopy. *Sci. Chin. Chem.* **2017**, *47*, 794–800.
24. Shang, G.; Li, C.; Wen, G.; Zhang, X.; Liang, A.; Jiang, Z. A new silver nanochain SERS analytical platform to detect trace hexametaphosphate with a rhodamine S molecular probe. *Luminescence* **2016**, *31*, 640–648. [CrossRef] [PubMed]
25. Li, C.; Wang, L.; Luo, Y.; Liang, A.; Wen, G.; Jiang, Z. A sensitive gold nanoplasmonic SERS quantitative analysis method for sulfate in serum using fullerene as catalyst. *Nanomaterials* **2018**, *8*, 277. [CrossRef] [PubMed]
26. Biesaga, M.; Schmidt, N.; Seubert, A. Coupled ion chromatography for the determination of chloride, phosphate and sulphate in concentrated nitric acid. *J. Chromatogr. A* **2004**, *1026*, 195–200. [CrossRef] [PubMed]

27. Ali, D.S.; Faizullah, A.T. Combination of FIA-CL technique with ion-exchanger for determination of sulphate in various water resources in Erbil City. *Arabian J. Chem.* **2012**, *5*, 147–153. [CrossRef]
28. Kumar, S.D.; Maiti, B.; Mathur, P.K. Determination of iodate and sulphate in iodized common salt by ion chromatography with conductivity detection. *Talanta* **2001**, *53*, 701–705. [CrossRef]
29. Meneses, S.R.; Maniasso, N.; Zagatto, E.A. Spectrophotometric flow-injection determination of sulphate in soil solutions. *Talanta* **2005**, *65*, 1313–1317. [CrossRef] [PubMed]
30. Fernández-Ramos, C.; Ballesteros, O.; Blanc, R. Determination of alcohol sulfates in wastewater treatment plant influents and effluents by gas chromatography-mass spectrometry. *Talanta* **2012**, *98*, 166–171. [CrossRef] [PubMed]